ILSim – A compact simulation tool for interferometric lithography

Yongfa Fan, Anatoly Bourov, Lena Zavyalova, Jianming Zhou, Andrew Estroff,
Neal Lafferty, Bruce W. Smith
Rochester Institute of Technology, Microelectronic Engineering Department
82 Lomb Memorial Drive, Rochester, NY 14623

ABSTRACT

Interference imaging systems are being used more extensively for R&D applications where NA manipulation, polarization control, relative beam attenuation, and other parameters are explored and projection imaging approaches may not exist. To facilitate interferometric lithography research, we have developed a compact simulation tool, ILSim, for studying multi-beam interferometric imaging, including fluid immersion lithography. The simulator is based on full-vector interference theory, which allows for application at extremely high NA values, such as those projected for use with immersion lithography. In this paper, ILSim is demonstrated for use with two-beam and four-beam interferometric immersion lithography. The simulation tool was written with Matlab, where the thin film assembly (ambient, top coat, resist layer, BARC layers, and substrate) and illumination conditions (wavelength, polarization state, interference angle, demodulation, NA) can be defined. The light intensity distributions within the resist film for 1 exposure or 2-pass exposure are displayed in the graph window. It also can optimize BARC layer thickness and top coat thickness.

Keywords: Interferometric lithography, High-NA, Modeling, Full vector imaging theory

1. INTRODUCTION

In a conventional lithographic imaging system, the patterns on the mask are projected through a set of lenses on a wafer coated with photoresist where the image of the patterns is recorded.[1] Interference lithography produces periodic patterns in a photoresist film by the interfering of two coherent laser beams. For a few special cases, diffraction-limited projection imaging is analogous to interference imaging. The first case is the projection imaging of a phase shifting grating mask (1:1 duty ration, alternating 180º phase, 100% transmission) with coherent illumination. The grating's 0^{th} diffraction order is zero. If the pitch of the grating is such that only the $\pm1^{st}$ diffraction orders are captured in the entrance pupil, the resulting image is simply the interference fringes of two plane waves with oblique angle θ (half of the angle subtended by the lens at the image plane). The second case is the projection imaging of a 1:1 binary grating mask with coherent illumination. If the pitch of the grating is such that only the 0^{th} and $\pm1^{st}$ diffraction orders are captured in the entrance pupil, the resulting image is the interference fringes of three plane waves, two beams with oblique angle θ, one normal to the image plane. The third case is the projection imaging of a 1:1 binary grating mask with off-axis coherent illumination. If the pitch of the grating is such that only the 0^{th} and one of the $\pm1^{st}$ diffraction orders are captured in the entrance pupil, the resulting image is the interference fringes of two plane waves of different amplitudes with oblique angle θ (since the amplitude of the 0^{th} order is different from that of the $\pm1^{st}$ orders). For the above cases with partial coherence illumination, the resulting images still can be considered as interference fringes but with weaker $\pm1^{st}$ diffraction orders since only part of the $\pm1^{st}$ orders is captured in the entrance pupil. In a word, imaging of the above grating objects from an optical projection system can be reduced to the problems of plane wave interference.

The resemblance of projection imaging to interference imaging in the cases analyzed in the preceding paragraph has stimulated studies of optical projection systems using an interferometric setup.[2] Although those are special cases, they represent a system's resolution limits, which mostly define the system's capability. An advantage of using an interferometric setup is that the costly lenses are not needed. At the same time, a single interferometric setup possesses the flexibility of emulating various lenses. The polarization of beams can be conveniently manipulated, allowing study of polarization effects. An extra flexibility is that the relative amplitude of the beams can be easily controlled. In view

of these advantages, a rigorous analysis of plane wave interference is performed in the following sections to afford a better understanding.

2. THEORY

2.1 Interference Imaging

Interference fringes will be formed in the intersection region of two or more sets of coherent monochromatic optical plane waves. Interference due to two or three polarized coherent monochromatic optical plane waves is analyzed here. The "beams" in the following discussion generally refer to monochromatic optical plane waves.

2.1.1 Two-beam interference with TE polarization

As illustrated in the Figure 2.1, two beams with equal oblique angle θ intersect at a plane. The electrical vectors of the plane waves are perpendicular to the plane of the figure (TE polarization). The intersection line is set as x axis with origin at the center of the beams. y axis is the normal direction. With the time dependence factor suppressed and the origin as phase reference point, the fields $\mathbf{E_1}$ (left beam) and $\mathbf{E_2}$ (right beam) at the intersection as a function of location x can be expressed respectively as,

$$\mathbf{E_1} = |\mathbf{E_1}|\mathbf{e}^{-\mathbf{i}(\mathbf{kx}\sin\theta)} \tag{1}$$

$$\mathbf{E_2} = |\mathbf{E_2}|\mathbf{e}^{-\mathbf{i}(-\mathbf{kx}\sin\theta)} \tag{2}$$

where k is the propagation vector, $\frac{2n\pi}{\lambda}$. The total field $\mathbf{E}$ at the intersection is the sum of the two,

$$\begin{aligned}\mathbf{E} = \mathbf{E_1} + \mathbf{E_2} &= |\mathbf{E_1}|e^{-i(kx\sin\theta)} + |\mathbf{E_2}|e^{-i(-kx\sin\theta)} \\ &= (|\mathbf{E_1}| + |\mathbf{E_2}|)\cos(kx\sin\theta) + i(|\mathbf{E_1}| - |\mathbf{E_2}|)\sin(kx\sin\theta)\end{aligned} \tag{3}$$

The corresponding intensity is proportional to the square of the amplitude of the field,

$$\begin{aligned}I \propto |\mathbf{E}|^2 &= |\mathbf{E_1} + \mathbf{E_2}|^2 \\ &= [(|\mathbf{E_1}| + |\mathbf{E_2}|)\cos(kx\sin\theta)]^2 + [(|\mathbf{E_1}| - |\mathbf{E_2}|)\sin(kx\sin\theta)]^2 \\ &= |\mathbf{E_1}|^2 + |\mathbf{E_2}|^2 + 2|\mathbf{E_1}||\mathbf{E_2}|\cos(2kx\sin\theta)\end{aligned} \tag{4}$$

The distribution of intensity along x direction is sinusoidal, the pitch (spatial period) of which is,

$$\mathbf{p} = \frac{\pi}{\mathbf{k}\sin\theta} = \frac{\lambda}{2\mathbf{n}\sin\theta} \tag{5}$$

For the phase shifting grating case discussed in the previous section, $|\mathbf{E_1}| = |\mathbf{E_2}|$, the intensity distribution is reduced to,

$$\mathbf{I} \propto 2|\mathbf{E_1}|^2[1 + \cos(2\mathbf{kx}\sin\theta)] = 4|\mathbf{E_1}|^2\cos^2(\mathbf{kx}\sin\theta) \tag{6}$$

For the case of binary grating with off axis illumination discussed in the previous section, $|\mathbf{E_2}| = \frac{1}{2\pi}|\mathbf{E_1}|$,[1] the intensity distribution is reduced to,

$$\mathbf{I} \propto |\mathbf{E_1}|^2[1 + \frac{1}{4\pi^2} + \frac{1}{\pi}\cos(2\mathbf{kx}\sin\theta)] \tag{7}$$

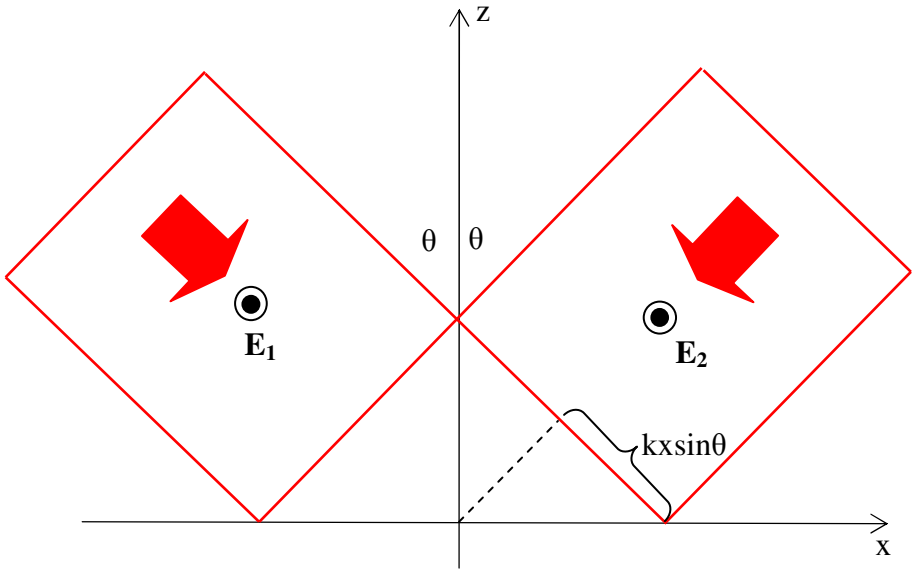

Fig. 2.1. Two monochromic plane waves with TE polarization intersect at a plane with equal oblique angle θ. The intersection line is set as x axis with origin at the center of the beams. y axis is the normal direction.

2.1.2 Two-beam interference with TM polarization

TM polarization refers to the polarization state where the electrical vectors of the plane waves are parallel to the plane of the figure, as illustrated in the Figure 2.2. For TE polarization, the total field is simply the scalar summation of the two plane waves since their electrical vectors are parallel to each other. For TM polarization, the electrical vector is a function of oblique angle θ, requiring vector operation for summation. $\mathbf{E_1}$ and $\mathbf{E_2}$ can be expressed respectively as,

$$\begin{aligned}\mathbf{E_1} &= \mathbf{E_{1x}}\hat{\mathbf{i}} + \mathbf{E_{1z}}\hat{\mathbf{j}} \\ &= |\mathbf{E_1}|\mathbf{e}^{-\mathbf{i}(\mathbf{kx}\sin\theta)}(\hat{\mathbf{i}}\cos\theta + \hat{\mathbf{j}}\sin\theta)\end{aligned} \tag{8}$$

$$\begin{aligned}\mathbf{E_2} &= \mathbf{E_{2x}}\hat{\mathbf{i}} + \mathbf{E_{2z}}\hat{\mathbf{j}} \\ &= |\mathbf{E_2}|\mathbf{e}^{-\mathbf{i}(-\mathbf{kx}\sin\theta)}(\hat{\mathbf{i}}\cos\theta - \hat{\mathbf{j}}\sin\theta)\end{aligned} \tag{9}$$

where $\hat{\mathbf{i}}$ and $\hat{\mathbf{j}}$ are unit vectors in x and z direction respectively, subscripts x, z designate x, z components of the electrical vectors. The total field $\mathbf{E}$ thus is,

$$\begin{aligned}\mathbf{E} &= \mathbf{E_1} + \mathbf{E_2} \\ &= (\mathbf{E_{1x}} + \mathbf{E_{2x}})\hat{\mathbf{i}} + (\mathbf{E_{1z}} + \mathbf{E_{2z}})\hat{\mathbf{j}} \\ &= (|\mathbf{E_1}|\mathbf{e}^{-\mathbf{i}(\mathbf{kx}\sin\theta)} + |\mathbf{E_2}|\mathbf{e}^{-\mathbf{i}(-\mathbf{kx}\sin\theta)})(\cos\theta)\hat{\mathbf{i}} + (|\mathbf{E_1}|\mathbf{e}^{-\mathbf{i}(\mathbf{kx}\sin\theta)} - |\mathbf{E_2}|\mathbf{e}^{-\mathbf{i}(-\mathbf{kx}\sin\theta)})(\sin\theta)\hat{\mathbf{j}} \\ \mathbf{E} &= [(|\mathbf{E_1}| + |\mathbf{E_2}|)\cos(\mathrm{kx}\sin\theta) + \mathrm{i}(|\mathbf{E_1}| - |\mathbf{E_2}|)\sin(\mathrm{kx}\sin\theta)](\cos\theta)\hat{\mathbf{i}} \\ &\quad + [(|\mathbf{E_1}| - |\mathbf{E_2}|)\cos(\mathrm{kx}\sin\theta) + \mathrm{i}(|\mathbf{E_1}| + |\mathbf{E_2}|)\sin(\mathrm{kx}\sin\theta)](\sin\theta)\hat{\mathbf{j}}\end{aligned} \tag{10}$$

The intensity distribution is evaluated as,

$$\begin{aligned}\mathbf{I} \propto |\mathbf{E}|^2 &= |\mathbf{E_1} + \mathbf{E_2}|^2 \\ &= |(\mathbf{E_{1x}} + \mathbf{E_{2x}})|^2 + |(\mathbf{E_{1z}} + \mathbf{E_{2z}})|^2 \\ &= [|\mathbf{E_1}|^2 + |\mathbf{E_2}|^2 + 2|\mathbf{E_1}||\mathbf{E_2}|\cos(2\mathbf{kx}\sin\theta)]\cos^2\theta + [|\mathbf{E_1}|^2 + |\mathbf{E_2}|^2 - 2|\mathbf{E_1}||\mathbf{E_2}|\cos(2\mathbf{kx}\sin\theta)]\sin^2\theta \\ &= |\mathbf{E_1}|^2 + |\mathbf{E_2}|^2 + 2|\mathbf{E_1}||\mathbf{E_2}|\cos(2\mathbf{kx}\sin\theta)(\cos^2\theta - \sin^2\theta) \\ \mathbf{I} &= |\mathbf{E_1}|^2 + |\mathbf{E_2}|^2 + 2|\mathbf{E_1}||\mathbf{E_2}|\cos(2\mathbf{kx}\sin\theta)\cos(2\theta)\end{aligned} \tag{11}$$

For the phase shifting grating case discussed in the previous section, $|\mathbf{E_1}| = |\mathbf{E_2}|$, the intensity distribution is reduced to,

$$I \propto 2|\mathbf{E_1}|^2[1+\cos(2kx\sin\theta)\cos(2\theta)] \tag{12}$$

For the case of binary grating with off axis illumination discussed in the previous section, $|\mathbf{E_2}| = \frac{1}{2\pi}|\mathbf{E_1}|$,[1] the intensity distribution is reduced to,

$$I \propto |\mathbf{E_1}|^2[1+\frac{1}{4\pi^2}+\frac{1}{\pi}\cos(2kx\sin\theta)\cos(2\theta)] \tag{13}$$

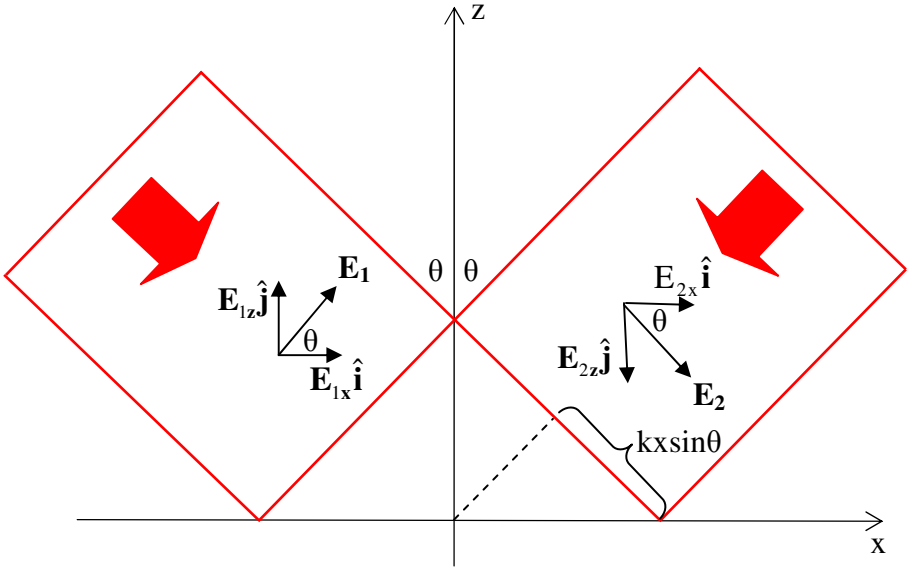

Fig. 2.2. Two monochromic plane waves with TM polarization intersect at a plane with equal oblique angle θ. The intersection line is set as x axis with origin at the center of the beams. z axis is the normal direction.

2.1.3. Three-beam interference with TE polarization

If there is a third beam $\mathbf{E_0}$ that is normal to the intersection of the two beams as discussed in the preceding sections, their interference can be analyzed in a similar way. Note that the beam $\mathbf{E_0}$ has a constant phase across the intersection. For TE polarization, the total field can be expressed as,

$$\begin{aligned}\mathbf{E} &= \mathbf{E_0}+\mathbf{E_1}+\mathbf{E_2}\\ &= |\mathbf{E_0}|+|\mathbf{E_1}|e^{-i(kx\sin\theta)}+|\mathbf{E_2}|e^{-i(-kx\sin\theta)}\\ &= |\mathbf{E_0}|+(|\mathbf{E_1}|+|\mathbf{E_2}|)\cos(kx\sin\theta)+i(|\mathbf{E_1}|-|\mathbf{E_2}|)\sin(kx\sin\theta)\end{aligned}$$

The intensity distribution therefore is,

$$\begin{aligned}I &\propto |\mathbf{E}|^2 = |\mathbf{E_0}+\mathbf{E_1}+\mathbf{E_2}|^2\\ &= |\mathbf{E_0}|^2+|\mathbf{E_1}|^2+|\mathbf{E_2}|^2+2|\mathbf{E_1}||\mathbf{E_2}|\cos(2kx\sin\theta)+2|\mathbf{E_0}|(|\mathbf{E_1}|+|\mathbf{E_2}|)\cos(kx\sin\theta)\end{aligned}$$

if $|\mathbf{E_1}| = |\mathbf{E_2}| = \frac{1}{2\pi}|\mathbf{E_0}|$,[1]

$$\mathbf{I} = (1+\frac{1}{2\pi^2})|\mathbf{E_0}|^2+\frac{1}{2\pi^2}|\mathbf{E_0}|^2\cos(2\mathbf{kx}\sin\theta)+\frac{2}{\pi}|\mathbf{E_0}|^2\cos(\mathbf{kx}\sin\theta) \tag{14}$$

2.1.4 Three-beam interference with TM polarization

Regarding to three-beam interference with TM polarization, the total field can be derived similarly,

$$
\begin{aligned}
\mathbf{E} &= \mathbf{E_0} + \mathbf{E_1} + \mathbf{E_2} \\
&= (\mathbf{E}_{0x} + \mathbf{E}_{1x} + \mathbf{E}_{2x})\hat{\mathbf{i}} + (\mathbf{E}_{0z} + \mathbf{E}_{1z} + \mathbf{E}_{2z})\hat{\mathbf{j}} \\
&= (\mathbf{E}_0 + \mathbf{E}_{1x} + \mathbf{E}_{2x})\hat{\mathbf{i}} + (\mathbf{E}_{1z} + \mathbf{E}_{2z})\hat{\mathbf{j}} \\
&= [|\mathbf{E_0}| + (|\mathbf{E_1}|\mathbf{e}^{-\mathbf{i}(\mathbf{kx}\sin\theta)} + |\mathbf{E_2}|\mathbf{e}^{-\mathbf{i}(-\mathbf{kx}\sin\theta)})(\cos\theta)]\hat{\mathbf{i}} + (|\mathbf{E_1}|\mathbf{e}^{-\mathbf{i}(\mathbf{kx}\sin\theta)} - |\mathbf{E_2}|\mathbf{e}^{-\mathbf{i}(-\mathbf{kx}\sin\theta)})(\sin\theta)\hat{\mathbf{j}} \\
&= [|\mathbf{E_0}| + (|\mathbf{E_1}| + |\mathbf{E_2}|)\cos(\mathbf{kx}\sin\theta)\cos\theta + \mathbf{i}(|\mathbf{E_1}| - |\mathbf{E_2}|)\sin(\mathbf{kx}\sin\theta)\cos\theta]\hat{\mathbf{i}} \\
&\quad + [(|\mathbf{E_1}| - |\mathbf{E_2}|)\cos(\mathbf{kx}\sin\theta) + \mathbf{i}(|\mathbf{E_1}| + |\mathbf{E_2}|)\sin(\mathbf{kx}\sin\theta)](\sin\theta)\hat{\mathbf{j}}
\end{aligned}
$$

The intensity distribution is:

$$
\begin{aligned}
\mathbf{I} \propto |\mathbf{E}|^2 &= |\mathbf{E_0} + \mathbf{E_1} + \mathbf{E_2}|^2 \\
&= |(\mathbf{E}_0 + \mathbf{E}_{1x} + \mathbf{E}_{2x})|^2 + |(\mathbf{E}_{1z} + \mathbf{E}_{2z})|^2 \\
&= |\mathbf{E}_0|^2 + [|\mathbf{E_1}|^2 + |\mathbf{E_2}|^2 + 2|\mathbf{E_1}||\mathbf{E_2}|\cos(2\mathbf{kx}\sin\theta)]\cos^2\theta + 2|\mathbf{E}_0|[(|\mathbf{E_1}| + |\mathbf{E_2}|)\cos(\mathbf{kx}\sin\theta)\cos\theta] \\
&\quad + [|\mathbf{E_1}|^2 + |\mathbf{E_2}|^2 - 2|\mathbf{E_1}||\mathbf{E_2}|\cos(2\mathbf{kx}\sin\theta)]\sin^2\theta \\
&= |\mathbf{E}_0|^2 + |\mathbf{E_1}|^2 + |\mathbf{E_2}|^2 + 2|\mathbf{E_1}||\mathbf{E_2}|\cos(2\mathbf{kx}\sin\theta)(\cos^2\theta - \sin^2\theta) + 2|\mathbf{E}_0|[(|\mathbf{E_1}| + |\mathbf{E_2}|)\cos(\mathbf{kx}\sin\theta)\cos\theta] \\
&= |\mathbf{E}_0|^2 + |\mathbf{E_1}|^2 + |\mathbf{E_2}|^2 + 2|\mathbf{E_1}||\mathbf{E_2}|\cos(2\mathbf{kx}\sin\theta)\cos(2\theta) + 2|\mathbf{E}_0|[(|\mathbf{E_1}| + |\mathbf{E_2}|)\cos(\mathbf{kx}\sin\theta)\cos\theta]
\end{aligned}
$$

if $|\mathbf{E_1}| = |\mathbf{E_2}| = \frac{1}{2\pi}|\mathbf{E}_0|$

$$
\mathrm{I} \propto (1 + \frac{1}{2\pi^2})|\mathbf{E}_0|^2 + \frac{1}{2\pi^2}|\mathbf{E}_0|^2\cos(2\mathrm{kx}\sin\theta)\cos(2\theta) + \frac{2}{\pi}|\mathbf{E}_0|^2\cos(\mathrm{kx}\sin\theta)\cos(\theta) \tag{15}
$$

2.2 Light propagation through a stack of thin films

2.2.1.Tranmission and reflection coefficients of a thin-film assembly

Transmission and reflection coefficients of a thin-film assembly can be computed using the well established thin-film matrix techniques based on Macleod's work.[3] The optical characteristic of a layer of thin film is expressed using a matrix,

$$
\mathbf{M_j} = \begin{bmatrix} \cos\delta_j & \mathbf{i}\sin\delta_j/\eta_j \\ \mathbf{i}\eta_j\sin\delta_j & \cos\delta_j \end{bmatrix} \tag{16}
$$

where δ_j is phase factor and η_j is the oblique optical admittance, which are defined respectively as,

$$
\eta_j = \mathbf{N_j}\cos\theta_j \quad \text{for TE polarization} \tag{17}
$$

$$
\eta_j = \frac{\mathbf{N_j}}{\cos\theta_j} \quad \text{for TM polarization} \tag{18}
$$

$$
\delta_j = \frac{2\pi\mathbf{d_j}\mathbf{N_j}\cos\theta_j}{\lambda} \tag{19}
$$

The characteristic matrix of an assembly with q layers is simply the product of the individual matrices,

$$
\begin{bmatrix} \mathbf{B} \\ \mathbf{C} \end{bmatrix} = \left(\prod_{j=1}^{j=q}\mathbf{M_j}\right)\begin{bmatrix} 1 \\ \eta_{\mathbf{sub}} \end{bmatrix} \tag{20}
$$

where subscript *sub* denotes the substrate.

The transmission and reflection coefficients of the thin film assembly are respectively expressed as,

$$
\tau = \frac{2\eta_0}{\mathbf{B}\eta + \mathbf{C}} \qquad\qquad \mathrm{r} = \frac{\mathrm{B}\eta_0 - \mathbf{C}}{\mathbf{B}\eta_0 + \mathbf{C}} \tag{21}
$$

where the oblique optical admittance in the incident media.

2.2.2. Intensity distribution within a thin film layer

A uniform medium is assumed in the preceding analysis on interference imaging. However, photoresist, the image recording media, is often in the form of a layer of thin film among an assembly of thin films. A typical film stack in modern lithography may include a top coat layer, a resist layer and a BARC (bottom antireflective coating) layer on a substrate. The top layer protects the resist layer by isolating it from the immersion fluid in the context of immersion lithography. The BARC layer functions to alleviate standing waves due to reflection from the substrate. The film stack forms an inhomogeneous medium. Reflections/refractions at the interfaces result in redistribution of light intensity within the photoresist layer. Donis George Flagello analyzed the light intensity distribution within the resist film which is on the top of the film stack.[4] When a top coat layer is present above the resist film, a similar analysis can be conducted to derive the light intensity distribution within the resist film.

A ray incident on the film stack is illustrated in Figure 2.3. The total field at any point within the resist layer is the sum of the downward field and upward field. The downward field and upward field at interface *X* are denoted as $\mathbf{E_{iX}}$ and $\mathbf{E_{rX}}$, respectively, where *X* is a Roman numeral for an interface. Then, the downward and upward fields at interface **III** are $\mathbf{E_{iII}}$ and $\mathbf{E_{rII}}$, respectively. The downward field and upward field at any point within the resist layer can be expressed as,

$$\begin{aligned}\mathbf{E}_{\downarrow} &= \mathbf{E_{iII}} e^{i\frac{2\pi \mathbf{N}_2}{\lambda}(\mathbf{d}_2-\mathbf{z})\cos\theta_2} \\ \mathbf{E}_{\uparrow} &= \mathbf{E_{rII}} e^{-i\frac{2\pi \mathbf{N}_2}{\lambda}(\mathbf{d}_2-\mathbf{z})\cos\theta_2}\end{aligned} \tag{22}$$

where *z* is the distance from interface **II**, the phase is referenced at interface **III**. The total field in the resist layer at any point *z* is therefore,

$$\begin{aligned}\mathbf{E}(\mathbf{z}) &= \mathbf{E}_{\downarrow} + \mathbf{E}_{\uparrow} \\ &= \mathbf{E_{iII}} e^{i\frac{2\pi \mathbf{N}_2}{\lambda}(\mathbf{d}_2-\mathbf{z})\cos\theta_2} + \mathbf{E_{rII}} e^{-i\frac{2\pi \mathbf{N}_2}{\lambda}(\mathbf{d}_2-\mathbf{z})\cos\theta_2}\end{aligned} \tag{23}$$

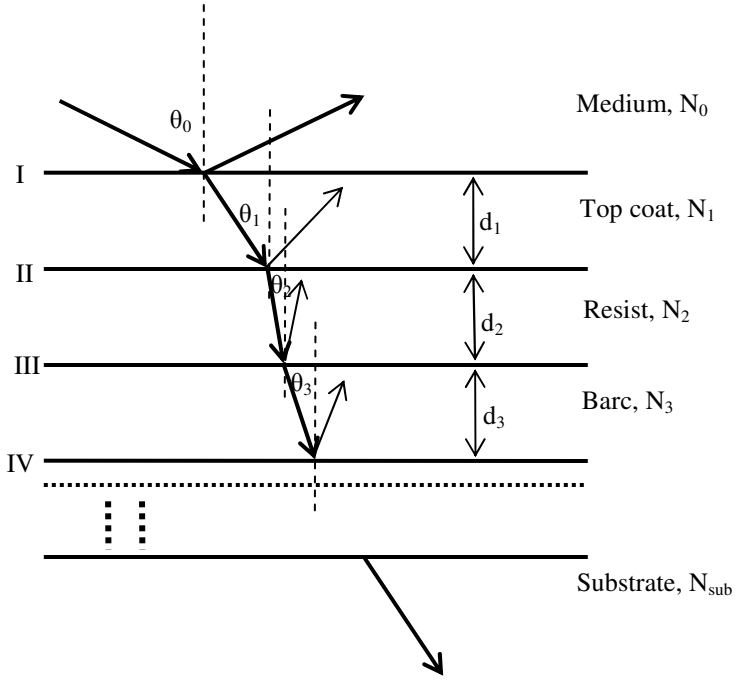

Fig. 2.3. Thin film stack on a substrate with incident plane wave. The film thicknesses, optical constants, interfaces, incident angles are denoted. The optical constants may be complex.

It can be shown that $\mathbf{E_{iII}}$ and $\mathbf{E_{rII}}$ are related to the incident field $\mathbf{E_{iI}}$ at interface **I**. The transmission and reflection coefficients at the interface **I** are defined as:

$$\boldsymbol{\tau_I} = \frac{\mathbf{E_{sub}}}{\mathbf{E_{iI}}} \qquad \mathbf{r_I} = \frac{\mathbf{E_{rI}}}{\mathbf{E_{iI}}} \tag{24}$$

where $\mathbf{E_{sub}}$ is the field transmitted at the last interface. Similarly, the transmission and reflection coefficients at interface **II**, **III** are defined as,

$$\boldsymbol{\tau_{II}} = \frac{\mathbf{E_{sub}}}{\mathbf{E_{iII}}} \qquad \mathbf{r_{II}} = \frac{\mathbf{E_{rII}}}{\mathbf{E_{iII}}} \tag{25}$$

$$\boldsymbol{\tau_{III}} = \frac{\mathbf{E_{sub}}}{\mathbf{E_{iIII}}} \qquad \mathbf{r_{III}} = \frac{\mathbf{E_{rIII}}}{\mathbf{E_{iIII}}} \tag{26}$$

From the above equations, the following relations can be derived,

$$\mathbf{E_{iIII}} = \frac{\boldsymbol{\tau_I}}{\boldsymbol{\tau_{III}}}\ \mathbf{E_{iI}} \qquad \mathbf{E_{rIII}} = \mathbf{r_{III}}\frac{\boldsymbol{\tau_I}}{\boldsymbol{\tau_{III}}}\ \mathbf{E_{iI}} \tag{27}$$

The total field **E**(z) at any point within the resist layer is derived by substituting the above equations into Equation (23),

$$\mathbf{E(z)} = \frac{\boldsymbol{\tau_I}}{\boldsymbol{\tau_{III}}}\ \left(\mathbf{e}^{\mathbf{i}\frac{2\pi \mathbf{N_2}}{\lambda}(\mathbf{d_2}-\mathbf{z})\cos\theta_2} + \mathbf{r_{III}}\mathbf{e}^{-\mathbf{i}\frac{2\pi \mathbf{N_2}}{\lambda}(\mathbf{d_2}-\mathbf{z})\cos\theta_2}\right)\mathbf{E_{iI}} \tag{28}$$

Further substitute of

$$\mathbf{F} = \frac{\boldsymbol{\tau_I}}{\boldsymbol{\tau_{III}}}\ \left(\mathbf{e}^{\mathbf{i}\frac{2\pi \mathbf{N_2}}{\lambda}(\mathbf{d_2}-\mathbf{z})\cos\theta_2} + \mathbf{r_{III}}\mathbf{e}^{-\mathbf{i}\frac{2\pi \mathbf{N_2}}{\lambda}(\mathbf{d_2}-\mathbf{z})\cos\theta_2}\right) \tag{29}$$

results in,

$$\mathbf{E(z)} = \mathbf{F}\mathbf{E_{iI}} \tag{30}$$

where **F** is termed as film function. It describes the standing-wave behavior due to the reflection from below the resist layer. Evaluation of F requires computing τ_I, τ_{III}, $r_{III,}$ which can be done using the Equation (21).

2.2.3 Film Function F

As discussed in the preceding section, the film function **F** describes the standing-wave effects within the resist layer due to reflection from the lower interface of the resist layer. From Equation (29), **F** can be evaluated using coefficients $\boldsymbol{\tau_I}$, $\boldsymbol{\tau_{III}}$ and $\mathbf{r_{III}}$, which are polarization dependent. For TE polarization, the film function **F** is simply expressed as,

$$\mathbf{F_S} = \left[\frac{\boldsymbol{\tau_I}}{\boldsymbol{\tau_{III}}}\right]_{\mathbf{S}}\ \left(\mathbf{e}^{\mathbf{i}\frac{2\pi \mathbf{N_2}}{\lambda}(\mathbf{d_2}-\mathbf{z})\cos\theta_2} + \left[\mathbf{r_{III}}\right]_{\mathbf{S}}\mathbf{e}^{-\mathbf{i}\frac{2\pi \mathbf{N_2}}{\lambda}(\mathbf{d_2}-\mathbf{z})\cos\theta_2}\right) \tag{31}$$

where the subscript S denotes TE (S) polarization. In the case of TM (P) polarization, the corresponding coefficients computed using standard thin film matrix techniques can not be applied to equation (30) directly in that a vector summation of the downward and upward fields is needed since their polarization directions are not parallel to each other. Decomposition of the incident electrical vector into x and z components which are then treated separately is necessary. The corresponding **F** functions are expressed as,

$$\mathbf{F_{xP}} = \left[\frac{\boldsymbol{\tau_I}}{\boldsymbol{\tau_{III}}}\right]_{\mathbf{xP}}\ \left(\mathbf{e}^{\mathbf{i}\frac{2\pi \mathbf{N_2}}{\lambda}(\mathbf{d_2}-\mathbf{z})\cos\theta_2} + \left[\mathbf{r_{III}}\right]_{\mathbf{xP}}\mathbf{e}^{-\mathbf{i}\frac{2\pi \mathbf{N_2}}{\lambda}(\mathbf{d_2}-\mathbf{z})\cos\theta_2}\right) \tag{32}$$

$$\mathbf{F_{zP}} = \left[\frac{\boldsymbol{\tau_I}}{\boldsymbol{\tau_{III}}}\right]_{\mathbf{zP}}\ \left(\mathbf{e}^{\mathbf{i}\frac{2\pi \mathbf{N_2}}{\lambda}(\mathbf{d_2}-\mathbf{z})\cos\theta_2} + \left[\mathbf{r_{III}}\right]_{\mathbf{zP}}\mathbf{e}^{-\mathbf{i}\frac{2\pi \mathbf{N_2}}{\lambda}(\mathbf{d_2}-\mathbf{z})\cos\theta_2}\right) \tag{33}$$

where subscripts x and z denote the related decomposition components. The coefficients $\boldsymbol{\tau_I}$, $\boldsymbol{\tau_{III}}$ and $\mathbf{r_{III}}$ of x components can be computed using standard thin film matrix techniques but not the z components. However, the relationship between the coefficients of x and z components can be established using Figure 2.4.

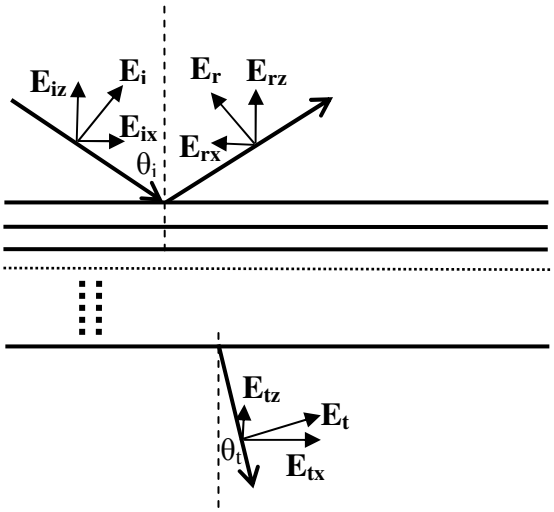

Fig. 2.4. A TM polarized incident wave incident on a stack of thin films with angle θ_i diffracts into a substrate with an angle θ_t. The electrical vectors are decomposed into x and z components.

As illustrated in Figure 2.4, a TM polarized incident wave incident on a stack of thin films with angle θ_i diffracts into a substrate with an angle θ_t. The electrical vectors of incident (denoted with subscript i) and diffracted waves (denoted with subscript t) are decomposed into x component (denoted with subscript x) and z component (denoted with subscript z). The reflection coefficient of x component is expressed as,

$$\mathbf{r_{xP}} = \frac{\mathbf{E_{rx}}}{\mathbf{E_{ix}}} \tag{34}$$

The z component is related to the x component by a simple tangent function. Also, it is noted that the $\mathbf{E_{rz}}$ is 180° out of phase with $\mathbf{E_{rx}}$. Therefore,

$$\mathbf{r_{zP}} = \frac{\mathbf{E_{rz}}}{\mathbf{E_{iz}}} = -\frac{\tan\theta_r \mathbf{E_{rx}}}{\tan\theta_i \mathbf{E_{ix}}} = -\frac{\mathbf{E_{rx}}}{\mathbf{E_{iz}}} = -\mathbf{r_{xP}}$$

$$\mathbf{r_{zP}} = -\mathbf{r_{xP}} \tag{35}$$

Similarly, the transmission coefficient of x component is expressed as,

$$\boldsymbol{\tau}_{\mathbf{xP}} = \frac{\mathbf{E_{tx}}}{\mathbf{E_{ix}}} \tag{36}$$

And the z component is related to the x component by a simple tangent function. Along with Snell's law, we have,

$$\boldsymbol{\tau}_{\mathbf{zP}} = \frac{\mathbf{E_{tz}}}{\mathbf{E_{iz}}} = \frac{\tan\theta_t \mathbf{E_{tx}}}{\tan\theta_i \mathbf{E_{ix}}} = \frac{\sin\theta_t \cos\theta_i \mathbf{E_{tx}}}{\sin\theta_i \cos\theta_t \mathbf{E_{iz}}} = \frac{\mathbf{N_i}\cos\theta_i \mathbf{E_{tx}}}{\mathbf{N_t}\cos\theta_t \mathbf{E_{iz}}}$$

$$\boldsymbol{\tau}_{\mathbf{zP}} = \frac{\mathbf{N_i}\cos\theta_i}{\mathbf{N_t}\cos\theta_t}\boldsymbol{\tau}_{\mathbf{xP}} \tag{37}$$

Application of the relationships from Equation (35) and (37) to Equation (33) yields the film function **F** for z component of TM polarization,

$$\mathbf{F_{zP}} = \frac{\mathbf{N_0}\cos\theta_0}{\mathbf{N_2}\cos\theta_2}\left[\frac{\boldsymbol{\tau}_{\mathbf{I}}}{\boldsymbol{\tau}_{\mathbf{III}}}\right]_{\mathbf{xP}} \left(\mathbf{e}^{\mathbf{i}\frac{2\pi \mathbf{N_2}}{\lambda}(\mathbf{d_2}-\mathbf{z})\cos\theta_2} - [\mathbf{r_{III}}]_{\mathbf{xP}} \mathbf{e}^{-\mathbf{i}\frac{2\pi \mathbf{N_2}}{\lambda}(\mathbf{d_2}-\mathbf{z})\cos\theta_2} \right) \tag{38}$$

Equation (31), (32) and (38) constitute the whole film function **F**. They are summarized here as:

$$\mathbf{F_S} = \left[\frac{\boldsymbol{\tau}_\mathbf{I}}{\boldsymbol{\tau}_\mathbf{III}}\right]_\mathbf{S} \left(\mathbf{e}^{\mathbf{i}\frac{2\pi \mathbf{N}_2}{\lambda}(\mathbf{d}_2-\mathbf{z})\cos\theta_2} + [\mathbf{r}_\mathbf{III}]_\mathbf{S} \mathbf{e}^{-\mathbf{i}\frac{2\pi \mathbf{N}_2}{\lambda}(\mathbf{d}_2-\mathbf{z})\cos\theta_2} \right) \tag{31}$$

$$\mathbf{F_{xP}} = \left[\frac{\boldsymbol{\tau}_\mathbf{I}}{\boldsymbol{\tau}_\mathbf{III}}\right]_\mathbf{xP} \left(\mathbf{e}^{\mathbf{i}\frac{2\pi \mathbf{N}_2}{\lambda}(\mathbf{d}_2-\mathbf{z})\cos\theta_2} + [\mathbf{r}_\mathbf{III}]_\mathbf{xP} \mathbf{e}^{-\mathbf{i}\frac{2\pi \mathbf{N}_2}{\lambda}(\mathbf{d}_2-\mathbf{z})\cos\theta_2} \right) \tag{32}$$

$$\mathbf{F_{zP}} = \frac{\mathbf{N}_0\cos\theta_0}{\mathbf{N}_2\cos\theta_2}\left[\frac{\boldsymbol{\tau}_\mathbf{I}}{\boldsymbol{\tau}_\mathbf{III}}\right]_\mathbf{xP} \left(\mathbf{e}^{\mathbf{i}\frac{2\pi \mathbf{N}_2}{\lambda}(\mathbf{d}_2-\mathbf{z})\cos\theta_2} - [\mathbf{r}_\mathbf{III}]_\mathbf{xP} \mathbf{e}^{-\mathbf{i}\frac{2\pi \mathbf{N}_2}{\lambda}(\mathbf{d}_2-\mathbf{z})\cos\theta_2} \right) \tag{38}$$

The light intensity distribution within the resist film resulting from interference is found simply by applying the film function **F** defined in the preceding paragraph. For example, applying film function **F** to Equation (6) and Equation (12), the intensity distributions within the resist film resulting from two-beam interference for TE and TM polarization are found respectively as,

$$\mathbf{I_{TE}} \propto 2|\mathbf{F_S}|^2|\mathbf{E_1}|^2[1+\cos(2\mathbf{kx}\sin\theta_0)] = 2|\mathbf{F_{TE}}|^2|\mathbf{E_1}|^2\cos^2(\mathbf{kx}\sin\theta_0) \tag{39}$$

$$\begin{aligned}
\mathbf{I_{TM}} &\propto |\mathbf{E}|^2 = |\mathbf{E_1}+\mathbf{E_2}|^2 \\
&= |(\mathbf{E_{1x}}+\mathbf{E_{2x}})|^2 + |(\mathbf{E_{1z}}+\mathbf{E_{2z}})|^2 \\
&= [|\mathbf{E_1}|^2+|\mathbf{E_2}|^2+2|\mathbf{E_1}||\mathbf{E_2}|\cos(2\mathbf{kx}\sin\theta_0)]\cos^2\theta_0 + [|\mathbf{E_1}|^2+|\mathbf{E_2}|^2-2|\mathbf{E_1}||\mathbf{E_2}|\cos(2\mathbf{kx}\sin\theta_0)]\sin^2\theta_0 \\
&= 2|\mathbf{F_{xP}}|^2|\mathbf{E_1}|^2\cos^2\theta_0[1+\cos(2\mathbf{kx}\sin\theta_0)] + 2|\mathbf{F_{zP}}|^2|\mathbf{E_1}|^2\sin^2\theta_0[1-\cos(2\mathbf{kx}\sin\theta_0)] \\
&= 4|\mathbf{F_{xP}}|^2|\mathbf{E_1}|^2\cos^2\theta_0\cos^2(\mathbf{kx}\sin\theta_0) + 4|\mathbf{F_{zP}}|^2|\mathbf{E_1}|^2\sin^2\theta_0\sin^2(\mathbf{kx}\sin\theta_0)]
\end{aligned} \tag{40}$$

$|\mathbf{F}|^2$ describes the standing wave effect in the vertical direction, which is not desirable in lithographic practice. It is convenient to express $\mathbf{r_{III}}$ in the form of

$$\mathbf{r_{III}} = |\mathbf{r_{III}}|\mathbf{e}^{\mathbf{i}\varphi} \tag{41}$$

where φ is a real number. Then film function Equation (29) becomes

$$\mathbf{F} = \frac{\boldsymbol{\tau}_\mathbf{I}}{\boldsymbol{\tau}_\mathbf{III}} \left(\mathbf{e}^{\mathbf{i}\frac{2\pi \mathbf{N}_2}{\lambda}(\mathbf{d}_2-\mathbf{z})\cos\theta_2} + |\mathbf{r_{III}}|\mathbf{e}^{-\mathbf{i}\left[\frac{2\pi \mathbf{N}_2}{\lambda}(\mathbf{d}_2-\mathbf{z})\cos\theta_2-\varphi\right]} \right)$$

Evaluation of $|\mathbf{F}|^2$ gives,

$$\begin{aligned}
|\mathbf{F}|^2 &= \left|\frac{\boldsymbol{\tau}_\mathbf{I}}{\boldsymbol{\tau}_\mathbf{III}}\right|^2 \left| \left(\mathbf{e}^{\mathbf{i}\frac{2\pi \mathbf{N}_2}{\lambda}(\mathbf{d}_2-\mathbf{z})\cos\theta_2} + |\mathbf{r_{III}}|\mathbf{e}^{-\mathbf{i}\left[\frac{2\pi \mathbf{N}_2}{\lambda}(\mathbf{d}_2-\mathbf{z})\cos\theta_2-\varphi\right]} \right) \right|^2 \\
&= \left|\frac{\boldsymbol{\tau}_\mathbf{I}}{\boldsymbol{\tau}_\mathbf{III}}\right|^2 \left| \left(1 + |\mathbf{r_{III}}|\mathbf{e}^{-\mathbf{i}\left[\frac{4\pi \mathbf{N}_2}{\lambda}(\mathbf{d}_2-\mathbf{z})\cos\theta_2-\varphi\right]} \right) \right|^2 \\
&= \left|\frac{\boldsymbol{\tau}_\mathbf{I}}{\boldsymbol{\tau}_\mathbf{III}}\right|^2 \left\{ 1 + |\mathbf{r_{III}}|^2 + 2|\mathbf{r_{III}}|\cos\left[\frac{4\pi \mathbf{N}_2}{\lambda}(\mathbf{d}_2-\mathbf{z})\cos\theta_2 - \varphi\right] \right\}
\end{aligned} \tag{42}$$

It indicates that the sinusoidal standing wave has a pitch of $\dfrac{\lambda}{2\,\mathrm{Re}(\mathbf{N}_2)\cos\theta_2}$. The amplitude of the standing wave is determined by $|\mathbf{r_{III}}|$. Complete suppression of the standing wave requires that r_{III} vanish.

3. INPUTS AND OUTPUTS SUMMARY

Based on the model described in the preceding section, a simulator called ILSim was built with Matlab for high NA modeling of interferometric lithography, allowing for image prediction and optimization. ILSIM's Inputs include optical constants for imaging media, thin films from the film stack and substrate, as well as imaging optics such as wavelength,

polarization, demodulation, propagation angle, numerical aperture, etc. The Outputs include the image in media, 2-D image in resist, 3-D image in resist, two-pass exposure images, reflection from top surface and substrate (BARC), etc. The inputs and outputs of ILSim were summarized in Table 1. The interactive interface to ILSim is used to define film stack data and imaging conditions. ILSim generates 2D and 3D intensity plot output for line/space patterns (two-and three-beam interference) and 'contact holes' (four- and five-beam interference).

Table 3.1. Summary of ILSim's inputs and outputs

ILSim Input	***ILsim Output***
Fluid properties	Image in media
Top coat	2D image in resist
Photoresist	3D image in resist
Multilayer BARCs	Two-pass exposure (top)
Substrate properties	Two-pass exposure (cross-section)
Wavelength	Polarized two-pass exposure
Polarization	Top Surface reflection
Demodulation	Substrate (BARC) reflection
Propagation angle	
Numerical aperture	

4. SIMULATION EXAMPLES

In this section, a number of simulation examples were given to illustrate various features of ILSim. The imaging optics conditions and film stack parameters are listed along with the simulation plots. In the plots, x, y and z are spacial coordinates with z denoting the depth into the resist.

4.1 Image in immersion media

The image in immersion media is the interferometric fringe in a uniform media in absence of a film stack. An example is shown in Figure 4.1 with the corresponding simulation parameters listed in Table 4.1.

Table 4.1 Simulation parameters for Example 4.1

Film Assembly		Optics	
Media	1.437	Wavelength	193 nm
Top coat	1.437	Polarization	TM
Resist	1.437	NA	1.05
Barc	1.437	Demodulation	0
Substrate	1.437		

4.2 2-D image in resist

The 2-D image in resist is the plot for iso-image contours. An example is shown in Figure 4.2.1 with the corresponding simulation parameters listed in Table 4.2. A simulation plot for the same simulation parameters but with TM polarization is shown in Figure 4.2.1.

Table 4.2 Simulation parameters for Example 4.2

Film Assembly		Optics	
Media	1.437	Wavelength	193 nm
Top coat	1.414, 40nm	Polarization	TE
Resist	1.71-0.0039i, 200nm	NA	1.2
Barc	1.82-0.34i, 39nm	Demodulation	0
Substrate	0.87-2.76i		

4.3 3-D image in resist
The 3-D image in resist is the surface plot for light intensity distribution within the resist. An example is shown in Figure 4.3 with the corresponding simulation parameters listed in Table 4.2.

4.4 Image contrast in resist
The image contrast in resist is plotted against the thickness of the resist. An example is shown in Figure 4.4 with the corresponding simulation parameters listed in Table 4.2 but with TM polarization.

4.5 2-Pass exposure with orthogonal/parallel polarization
The wafer is exposed once, then it is turned 90 degree for a second-pass exposure. If the polarization direction remains the same for the second exposure, it is called orthogonal polarization 2-pass exposure configuration. If the polarization direction is turned 90degree for the second exposure, it is called parallel polarization 2-pass exposure configuration. The iso-image contours of a top-down view or cross-section of the resist can be simulated as illustrated in Figure 4.5.1 and Figure 4.5.2. The corresponding simulation parameters listed in Table 4.2.

4.6 Reflection from top surface and substrate (BARC)
The reflection from the top surface and the substrate (BARC) as a function of top layer thickness or BARC thickness can be simulated for optimal thickness. An example is shown in Figure 4.6.1 and Figure 4.6.2. The reflection for both TE and TM is shown. An optical thickness for TE polarization is shown in the plot. The corresponding simulation parameters listed in Table 4.2.

5. CONCLUSION

A compact simulation tool, ILSim, was built for studying multi-beam interferometric imaging, including fluid immersion lithography. The tool is based on the full-vector interference theory, allowing for application at extremely high NA values, such as those projected for use with immersion lithography. The thin film assembly (ambient, top coat, resist layer, BARC layers, and substrate) and illumination conditions (wavelength, polarization state, interference angle, demodulation, NA) can be defined in the interactive interface. Various simulations examples were demonstrated. ILSim is a useful simulation tool for interferometric lithography

6. REFERENCES

1. B. W. Smith, “Optics for Photolithography,” in *Microlithography Science and Technology*, J. R. Sheats, B. W. Smith, eds. (Marcel Dekker, 1998) , pp171-270.
2. F. Cropanese, A. Bourov, Y. Fan, A. Estroff, L. Zavyalova, “Synthesis of projection lithography for low k1 via interferometry”, in *Optical Microlithography XVII*, B. W. Smith ed., Proc. SPIE , **5377**, PART 3, 1836-1842 (2004).
3. H. A. Macleod, *Thin-film optical filters* (Macmillan Publishing Company, 1985).
4. D. G. Flagello, “High numerical aperture imaging in homogeneous thin fims”, Ph.D. Dissertation, University of Arizona, 1993

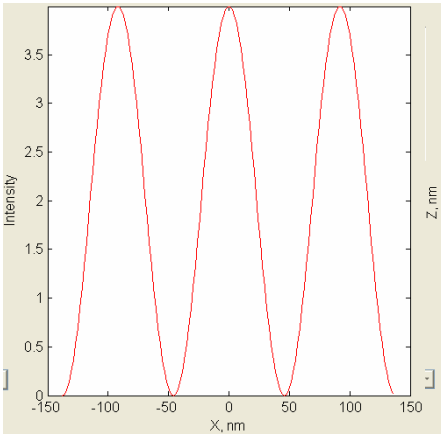

Fig. 4.1 Image in immersion media.

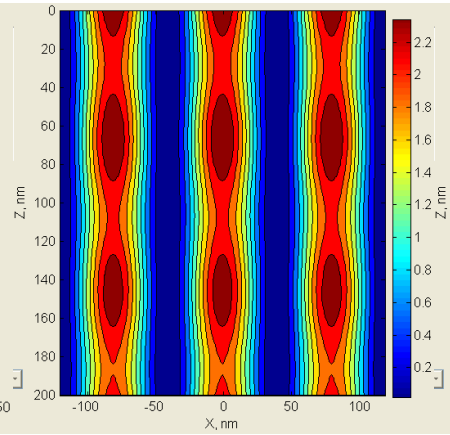

Fig. 4.2.1 2-D image in resist.

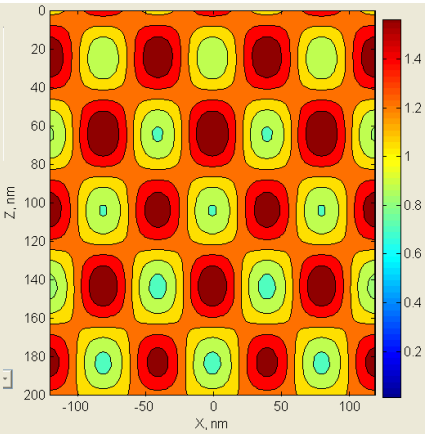

Fig. 4.2.2 2-D image in resist.

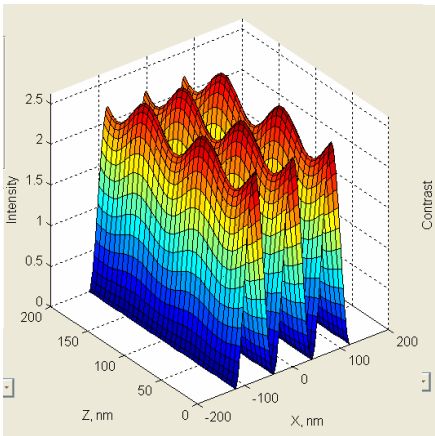

Fig. 4.3 3-D image in resist.

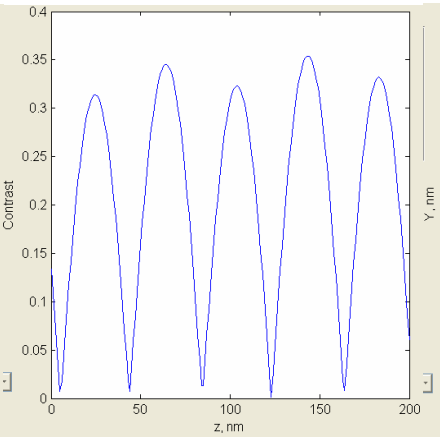

Fig. 4.4 Image contrast in resist.

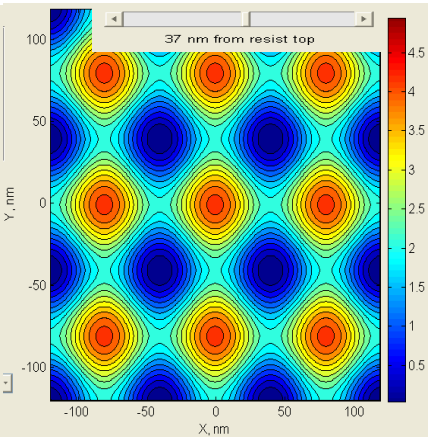

Fig. 4.5.1 2-Pass, orthogonal pol., top down.

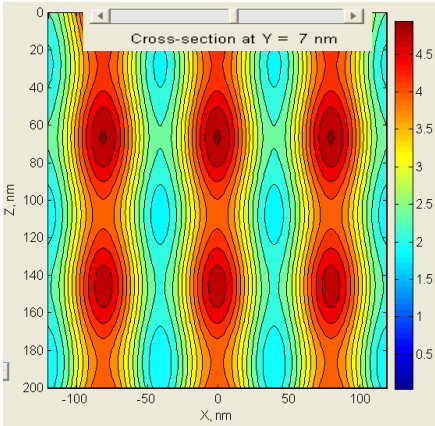

Fig.4.5.2 2-Pass, orthogonal pol., cross-section.

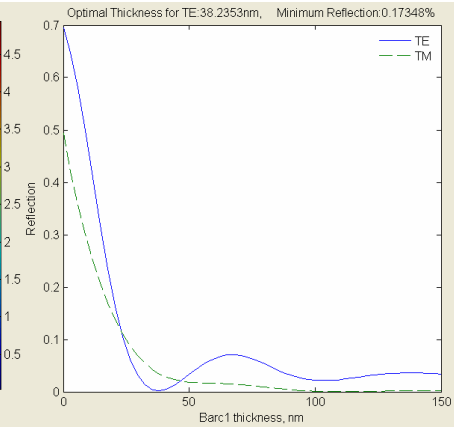

Fig.4.6.1 Substrate (BARC) reflection.

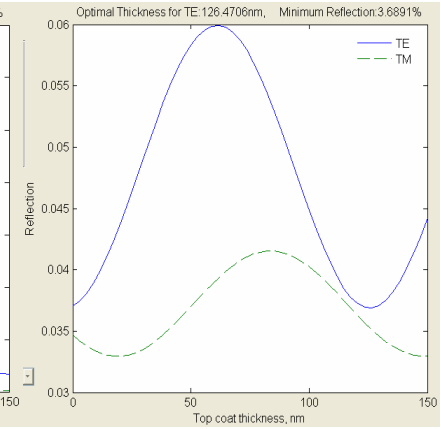

Fig.4.6.2 Top surface reflection.